AIP Journal of Applied Physics

A correlation force spectrometer for single molecule measurements under tensile load

Milad Radiom, Christopher D. F. Honig, John Y. Walz, Mark R. Paul, and William A. Ducker

Citation: Journal of Applied Physics **113**, 013503 (2013); doi: 10.1063/1.4772646
View online: http://dx.doi.org/10.1063/1.4772646
View Table of Contents: http://scitation.aip.org/content/aip/journal/jap/113/1?ver=pdfcov
Published by the AIP Publishing

A correlation force spectrometer for single molecule measurements under tensile load

Milad Radiom,[1] Christopher D. F. Honig,[1] John Y. Walz,[1] Mark R. Paul,[2] and William A. Ducker[1,a)]
[1]*Department of Chemical Engineering, Virginia Tech, Blacksburg, Virginia 24060, USA*
[2]*Department of Mechanical Engineering, Virginia Tech, Blacksburg, Virginia 24060, USA*

(Received 30 October 2012; accepted 29 November 2012; published online 2 January 2013)

The dynamical-mechanical properties of a small region of fluid can be measured using two closely spaced thermally stimulated micrometer-scale cantilevers. We call this technique correlation force spectroscopy (CFS). We describe an instrument that is designed for characterizing the extensional properties of polymer molecules that straddle the gap between the two cantilevers and use it to measure the stiffness and damping (molecular friction) of a dextran molecule. The device is based on a commercial atomic force microscope, into which we have incorporated a second antiparallel cantilever. The deflection of each cantilever is measured in the frequency range dc–1 MHz and is used to generate the cross-correlation at equilibrium. The main advantage of cross-correlation measurements is the reduction in thermal noise, which sets a fundamental noise limit to force resolution. We show that the thermal noise in our cross-correlation measurements is less than one third of the value for single-cantilever force microscopy. The dynamics of the cantilever pair is modeled using the deterministic motion of a harmonic oscillator initially displaced from equilibrium, which yields the equilibrium auto and cross-correlations in cantilever displacement via the fluctuation-dissipation theorem. Fitted parameters from the model (stiffness and damping) are used to characterize the fluid at equilibrium, including any straddling molecules. © *2013 American Institute of Physics*. [http://dx.doi.org/10.1063/1.4772646]

I. INTRODUCTION

Correlations in the thermal fluctuations of micron scale objects in fluid have been used to study the microrheology of fluids and the spectroscopy of single molecules.[1–10] In microrheology, very good progress has been made using the dual trap optical tweezers technique;[8,11,12] however, the technique has a limited frequency range, requires large particle-particle separation, and it is most effective for systems with elastic moduli <100 Pa.[13] We have developed a device, the correlation force spectrometer (CFS), which is capable of measurement of fluid properties on length scales of micrometers to nanometers at frequencies up to 1 MHz.[14] This device consists of a pair of micrometer-scale cantilevers that are closely spaced, and two optical lever detection systems to measure the thermally excited vibrations of each cantilever. The vibrations of the two cantilevers are not independent, but are coupled through the fluid and any straddling molecules. Measurement and analysis of the correlations between the displacements of the two cantilevers can be used to quantify the nature of this coupling, and therefore to determine the properties of the fluid and straddling molecules. Since cantilevers of various stiffness can be used, it is possible to measure the elastic response of materials with a large range of elastic moduli (from very soft "viscous-like" materials to strong elastic materials).

The dual trap optical tweezers technique has also been used to measure the mechanical properties of single molecules.[15–20] Comparing the dual trap technique with atomic force microscopy (AFM) single molecule force spectroscopy,[21–25] the dual trap technique has much lower noise, partly because uncorrelated noise in the motion of each probe does not contribute to the cross-correlation. It would be advantageous to AFM single-molecule measurements if the cross-correlation measurement that has been so successful in the dual trap optical tweezers technique could be implemented in AFM: that is the purpose of the current paper. In particular, here we implement the two AFM cantilevers in a vertical offset configuration (Fig. 1(b)) rather than the laterally offset configuration described previously.[14] In the new vertical-offset instrument, (a) the straddling molecules are strained in an extensional mode (rather than in a shear mode), (b) the average separation between the cantilevers can be varied, and (c) we retain the full scanning capability of an AFM.

The main advantage of measuring cross-correlations rather than deflections is the low noise. In particular, the *thermal noise* is reduced. This is particularly important in biomolecular studies because many biomolecular events have an energy similar to the thermal noise.[26] For a cantilever of spring constant $k \sim 0.1$ N/m, the thermal noise of a single cantilever sets a bound on the force noise amplitude of order $\sqrt{kk_BT} \sim 20$ pN where k_B is the Boltzmann constant and T is the temperature. One possibility to reduce this noise is to reduce the cantilever spring constant by reducing the dimensions of the cantilever uniformly to yield, for example, a nanocantilever. A significant detractor to this approach is that the cantilever dynamics become overdamped as the viscous forces dominate the cantilever inertia.[5]

a)Electronic mail: wducker@vt.edu.

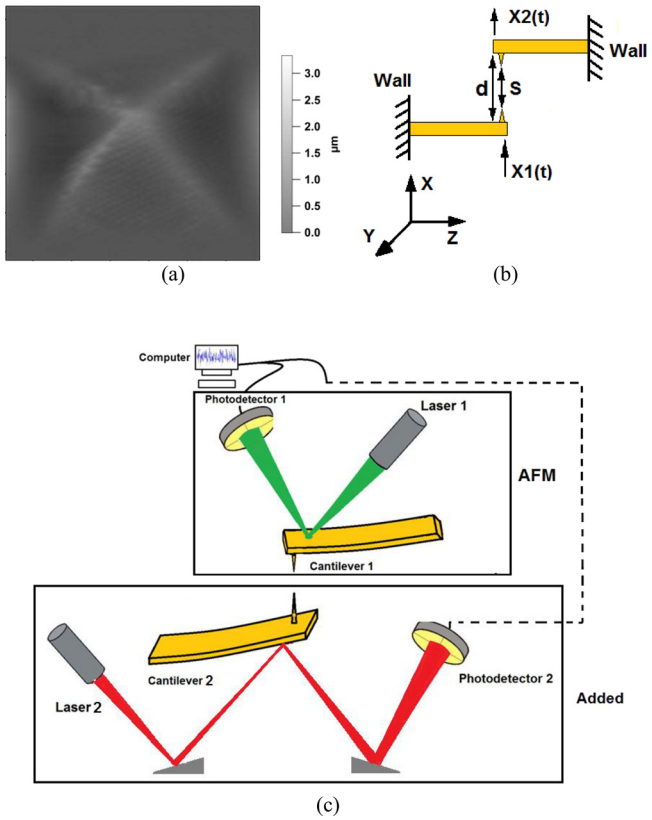

FIG. 1. (a) Atomic force microscopy contact mode image in water of the bottom cantilever tip obtained by scanning the bottom cantilever and measuring the height signal. This imaging is used to align the tips. (b) Schematic of antiparallel vertically offset cantilevers. The cantilevers are 200 μm long and 40 μm wide and the tip is 3.1 μm high (h), thus we have: $d = s + 2h$. (c) Schematic of the cantilevers and detection system in the antiparallel vertically offset CFS. The ends of the real cantilevers are tapered with an angle of approximately 59°.

Note that the thermal noise arises from interactions of the entire cantilever with the immersion fluid. In contrast, the cross-correlation of the thermal noise between two cantilevers only arises from the region where the two cantilevers interact, so we effectively reduce noise by sampling a smaller region of the cantilever. Later, we will show experimentally that the cross-correlated noise is much smaller than the noise on a single cantilever.

In a one-cantilever single molecule force spectroscopy experiment, a polymer molecule is stretched between a plate and a sharp tip by a cantilever.[26] The polymer stiffness is measured from the cantilever deflection at a finite loading rate. These experiments have been successful, but they examine polymers in a highly stretched state. Measurement of the thermal fluctuations has the advantage that a weaker loading and the molecular dissipation can be measured, as demonstrated by Smith and McLeish.[27–29] Here, we go one step further and measure the correlations in fluctuations of two cantilevers.

We also emphasize that bringing a micron-scale cantilever near to a plate significantly reduces both the resonant frequency and the quality factor because of the damping introduced by confining water in the thin film near the plate.[30,31] When we measure the dissipation between two AFM tips, there is no plate, allowing measurement at higher resonant frequency and quality than the tip–plate configuration. This reduces the background damping, against which polymer damping must be measured.

In this paper, we start by describing the instrument, and then show experimental measurements of correlations in the thermal fluctuation of a cantilever pair as a function of separation between the cantilevers in water. Understanding the motion of the cantilever in water, for the precise conditions of experiment, is a necessary precursor to understanding the motion of an added molecule spanning the gap between the cantilevers. We then characterize the hydrodynamic damping using a simple harmonic oscillator (HO) model. The HO model allows us to parameterize fluid and cantilever properties. A single molecule of dextran is then made to span between the AFM cantilever tips and the fluctuations are remeasured. We are then able to characterize the polymer with the additional parameters, polymer damping and stiffness, that are fitted to the correlated fluctuations.

II. MATERIALS AND METHODS

The apparatus consists of a pair of commercial AFM cantilevers (ORC8 type B, Brucker, CA) mounted in an antiparallel vertically offset configuration as shown schematically in Fig. 1. The top cantilever is mounted in a commercial AFM (Asylum Research, MFP3D-bio, CA) that has the full functionality of AFM, such as sub-nm resolution in deflection and displacement in three dimensions. A home-built cantilever mount and optical lever detector[32] was incorporated into the AFM in place of "the sample." For this additional cantilever deflection sensor, a laser (Schäfter + Kirchhoff GmbH, Hamburg, Germany, 51nanoFCM) is steered by a mirror onto the cantilever and the reflection off the cantilever falls onto a second mirror which then steers the beam onto a split photodiode (Pacific Silicon Sensor, CA, QP50-6-18u-SD2). We use a different wavelength (680 nm) of laser for the bottom cantilever compared to the top cantilever (Superluminescent diode with an 860 nm wavelength) to allow frequency filtering, thereby preventing optical contamination of the two signals. The two laser beams are also physically separated so that they do not contaminate each other. The main danger of unwanted cross-correlation (that does not arise from the fluid) is from light from a single laser that ends up striking both cantilevers and entering a single diode. This could occur if the cantilevers are parallel and if the laser beam is larger than the cantilever or the cantilever allows transmission of light. We try to cover all these possibilities by using standard gold coatings on the cantilevers, by focusing the laser beams to a spot size that is smaller than the cantilever (spot size ~12 μm), and by not making the cantilevers perfectly parallel. We use the absence of a cross-correlation at zero time lag in water as our requirement for no instrumental cross-talk between the signals.

The experimental procedure is as follows. A fluid droplet is injected and held in place by capillary action and the system is left to reach equilibrium for about 40 min. Initially, while the cantilevers are at large separation, the power spectral density (PSD) of each cantilever is measured and a

Lorentzian fit is applied to PSDs to yield the resonant frequency and quality factor of and therefore the damping coefficient, γ_a, of each cantilever at infinite separation. The same data are later used to calculate the spring constant of each cantilever.

The tips are then brought near each other using the course z-control in the AFM, and then aligned more precisely by imaging the bottom cantilever with the top cantilever. Note that the entire detection system (cantilever, laser and diode) is scanned to maintain the alignment of the detection system on the cantilever. The Asylum AFM has a convenient "go there" function where the sample can be moved automatically to a location within a previously collected image. We use this function to move the top AFM tip to the apex of the bottom tip.

To determine the spring constant, and for later reporting of cantilever deflection, we also need to know the deflection of the cantilevers in units of distance, rather than in voltage from the photodiode. The calibration is very similar to the traditional method in AFM:[33] The two cantilevers are brought into contact (as in Fig. 2) and a single force-extension measurement is performed. Referring to the schematic in Fig. 1(c), we do this by translating the right end of the top cantilever downward a known distance with the z-piezo and measuring the uncalibrated deflection of *each* cantilever in units of volts. When the tips are in contact, the combined deflection in nanometers is equal to the distance travelled by the z-piezo.

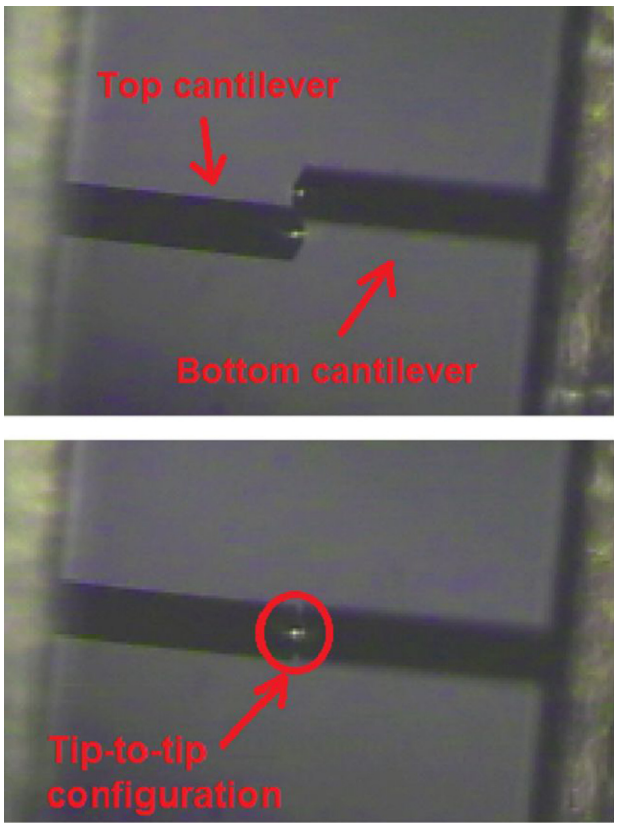

FIG. 2. Top view optical microscope images of the cantilever pair. (Top) The two cantilevers are brought in proximity of each other. (Bottom) The two cantilevers are aligned coarsely using micrometer translation stage and then with nanometer precision using the piezoelectric devices of the AFM.

We use a pair of cantilevers from the same wafer and assume that the cantilevers have identical spring constants, and therefore the deflection in volts of each cantilever is equal to half the translation by the z-piezo. We justify this assumption by noting that the resonant frequencies and quality factors of the two cantilevers are very similar. The calibration for deflection (InvOLS) is then half of the slope of the voltage–z-piezo plot. If the cantilevers were to have different spring constants, then we would use the appropriate weighting to determine the InvOLS.

An alternative method for calibrating the InvOLS would be to first calibrate the deflection of a single cantilever by pressing it against a solid, and then substituting the second cantilever for the solid. However, the InvOLS depends on the immersion fluid and the laser alignment, and in our current apparatus, it is difficult to exchange samples within a fluid.

Periodically, a new image can be taken to realign the horizontal position of the tips and re-establish the vertical separation zero position between the two tips. This is necessary to account for any drift in position. Once this is done, the z-piezo can be used to establish the required separation in z. With the tips in alignment, the z-piezo can be used to select a vertical tip-to-tip separation. From this point, and during data collection there are no "moving" parts; the only motion is molecular motion of the fluid and the fluctuating deflection of the cantilevers due to motion of the molecules within the fluid and cantilever.

The signals from the top cantilever (part of the commercial AFM) and the bottom cantilever are recorded synchronously by an Asylum Research Atomic Force Microscope controller (Nyquist frequency, $f_{\mathrm{Ny}} = 25$ kHz) or a National Instrument (Irvine, CA) NI PCI-6110 Data Acquisition card ($f_{\mathrm{Ny}} = 500$ kHz). The phase lag between detection systems was shown to be negligible in an experiment when both lasers recorded the motion of a single cantilever. By measurement of the energy spectral density as a function of laser power, we found that the laser had a negligible effect on the temperature of the cantilever. The energy spectral density did not change noticeably between the beginning and the end of the experiment, indicating that the cantilevers were not damaged during the course of the experiment (from laser power or adsorption of contaminants).

In each experiment, we typically measure the deflection signals at 50 kHz for 50 s or 1 MHz for 16 s. Subsequent data processing consists of (1) dividing the data points into N bins, (2) subtracting a linear curve fit from each bin to remove drift in the signal (this removes the deflection of the AFM cantilevers that arises from small temperature changes), (3) taking a Fourier transform of each bin and calculating the PSD for each cantilever averaged over all bins, and (4) normalizing the data by dividing through by $\sqrt{A/f_{Ny}}$ where A is the area under the PSD. The noise spectra are then $G_{11}(\omega) = \frac{1}{N}\sum_{\mathrm{bins}} \widehat{x}_1(\omega)\widehat{x}_1^*(\omega)$ and $G_{12}(\omega) = \frac{1}{N}\sum_{\mathrm{bins}} \widehat{x}_1(\omega)\widehat{x}_2^*(\omega)$ where $\widehat{x}_i(\omega)$ is the Fourier transform of the normalized signal from each cantilever and ω is the frequency. The cross-correlation is normalized by the geometric mean of the normalization constant for each contributing signal.

The auto and cross-correlation functions are then the inverse Fourier transform of the noise spectra for which we used an inverse fast Fourier transform function: $\langle x_i(t)x_j(0)\rangle' = \text{IFFT}\ (G_{ij})$ where $i = j$ for autocorrelation and $i \neq j$ for cross-correlation. The superscript on the correlation function $\langle \ldots \rangle'$ denotes normalized calculations. The normalization procedure described in step (4) gives a value of the autocorrelation of unity at zero time lag: $\langle x_i(t)x_i(0)\rangle' = 1$.

III. RESULTS AND DISCUSSION

A principal advantage of two cantilever measurements (CFS) over one cantilever measurements is that the thermal noise in the cross-correlations between the two cantilevers is much smaller than the thermal noise in the autocorrelation (for a single cantilever).[34] This principal has already been demonstrated in dual trap optical tweezers measurements,[1,15] and theoretically for a cantilever pair.[35] The power density spectrum of the autocorrelation and cross-correlation of the deflection in our CFS is shown in Fig. 3. It is clear that the cross-correlation noise spectrum has a much smaller magnitude and is typically about 1/4 of the autocorrelation noise spectrum for the same cantilever in the same fluid at this value of the cantilever separation. When molecules are studied by straddling them between the cantilevers, this cross-correlation arising from the solvent coupling of the cantilevers will be the "noise" that sets the limit of force resolution. Thus, by changing from one cantilever to two cantilever measurements, we have lowered a fundamental noise limit in AFM single molecule spectroscopy. The dispersion of noise in the cross-correlation also has the interesting feature that there is a particular frequency near the resonant frequency where the thermal noise is zero (see Fig. 3).

The autocorrelations and cross-correlations of the deflections of the cantilevers at various separations in water are shown in Fig. 4. The autocorrelation is a very weak function of separation. In contrast, the magnitude of the cross-correlation increases monotonically as the tips are brought closer together. This is expected: The fluid coupling is stronger when the tips are closer together.[3] A similar effect has been observed for two particles using the optical tweezers technique.[36]

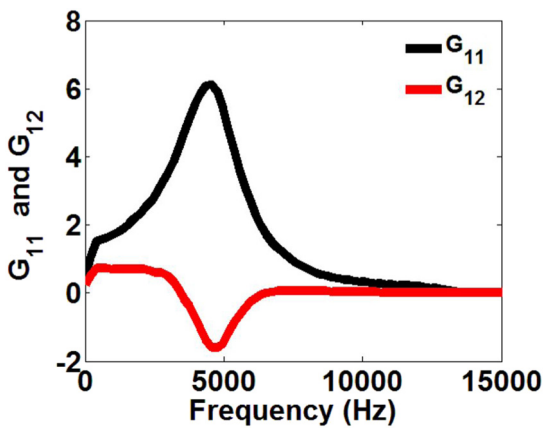

FIG. 3. Comparison between the normalized power spectral density (G_{11}) and the normalized cross-correlation noise spectrum (G_{12}) in water at 23 °C (ORC8 B: length = 200 μm, width = 40 μm, k = 0.1 N m^{-1}). Separation between the cantilevers is $d = 6.5$ μm ($s = 318$ nm).

The change in cross-correlation with separation also demonstrates that the observed correlation arises from the fluid coupling in the tiny gap between the cantilevers, and not from a spurious external driving of the entire device by a noise source in our lab.

The cross-correlation does not change significantly at smaller cantilever separations ($d = 6.5$–7.2 μm), which corresponds to smaller tip separations ($s = 318$–1000 nm). At this point, we do not have a complete understanding of why the cross-correlation does not change significantly in this range, but we do note that this separation of less than 1 μm is much less the size of the unsteady viscous boundary layer around the oscillating cantilever. This boundary layer is approximately given by the Stokes length, $\delta_s = \sqrt{\upsilon/\omega_r}$ where υ is the kinematic viscosity. For our apparatus, the Stokes length is approximately 14 μm for ORC8-B cantilever in water. Thus, the two cantilevers are well within the viscous dominant region of the flow. We note that the overlap in the cantilevers is about 8 μm × 40 μm (Figs. 1(b) and 2), which is much greater than the area of the tips, so it is not surprising that the hydrodynamics is dominated by the cantilevers and not the tips. The important point is that the coupling is very weakly dependent on the tip-tip separation. The insensitivity of the background "noise" to tip separation will be a very useful property in single-molecule studies because the modeling of the noise can be held constant while molecules are subject to different extensions and compressions by the tips.

Figure 4 also shows that during the time span of 0 to 0.5 ms there are several in-phase and out-of-phase correlations in thermal fluctuations of the two cantilevers. This behavior is different from the behavior of two particles trapped in an optical trap where only one anti-correlation can be seen over 0 to 4 ms,[1] because of the lower Q. This shows the capability of CFS to give more detailed information over a shorter time span.

Note that because the instrument is based on a commercial AFM, the separation s between the tips changes with time (drifts) even when the voltage to the piezo is kept constant. This drift primarily arises from changes in temperature that cause the dimensions of all parts of the apparatus to change with time, and in particular, the parts that rigidly link the two tips. This drift changes the separation, s, between the tips in an unknown way. The cantilevers, which consist of silicon nitride with a gold coating, tend to bend slightly with small temperature, which also changes s. In contrast, movements of the piezo are reliably known because they are measured independently by a linear variable differential transducer, so we measure the separation using the piezo. The separations shown in Fig. 4 were obtained by extending the z-piezo so that the tips touched each other, then retracting the piezo to the desired position, measuring the auto and cross-correlation, and then again extending the z-piezo to touch the tips. Each value of s is the average distance travelled before and after the correlations are measured. The distance before and after varied by up to 200 nm which shows the extent of the drift during this measurement.

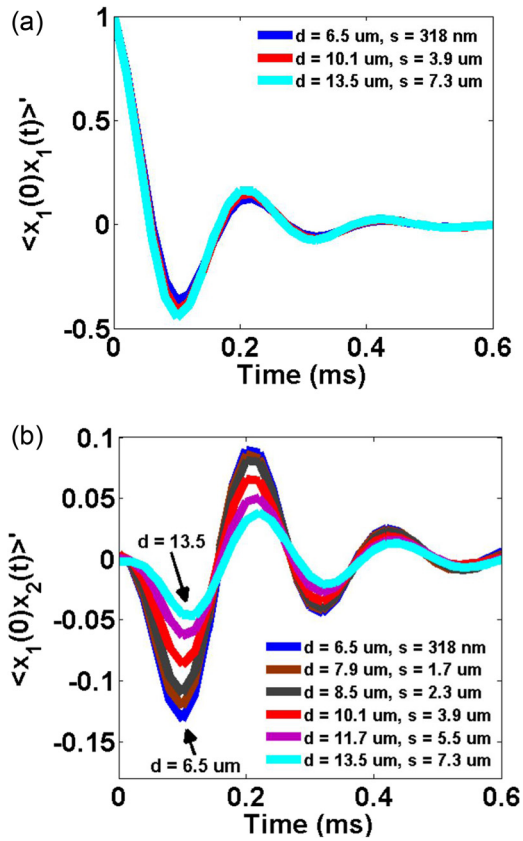

FIG. 4. (a) Autocorrelation and (b) cross-correlation of equilibrium fluctuations in cantilever deflection in water at 23 °C. A series of measurements is shown for various tip–tip separations, $s = 318$–7300 nm, which corresponds to a cantilever–cantilever separation, $d = 6.5$–$13.5\ \mu$m. $d = 6.5\ \mu$m and $d = 13.5\ \mu$m are labeled and the rest of separations are in sequential order. Commercial AFM cantilevers are used (ORC8 B: length $= 200\ \mu$m, width $= 40\ \mu$m, k $= 0.1$ N m^{-1}). The prime on the left axis indicates normalized correlation function. Note that the autocorrelation data for different separations almost overlay: There is a slight decrease in amplitude at smaller separations. The cross-correlation increases monotonically as the separation decreases. Discrete points have been represented as a line for clarity.

IV. MODELING THE CORRELATIONS IN WATER

The first stage of the analysis is the realization that the thermally driven oscillations that we measure have the same origin as the decay of the system with time, starting from a non-equilibrium condition. If the initial condition is close to equilibrium, the response will be linear and we can invoke the fluctuation-dissipation theorem,[37] and model the thermal fluctuations with a deterministic ringdown of the cantilever as described by Paul and Cross.[5,38]

The autocorrelation, $\langle x_1(0)x_1(t)\rangle$, and cross-correlation, $\langle x_1(0)x_2(t)\rangle$, of equilibrium fluctuations in cantilever tip displacement are given by the deterministic ringdown of the cantilevers due to the removal of a step force from the free end of one of the cantilevers[35]

$$\langle x_1(0)x_1(t)\rangle = \frac{k_B T}{F_1} X_1(t), \tag{1}$$

$$\langle x_1(0)x_2(t)\rangle = \frac{k_B T}{F_1} X_2(t), \tag{2}$$

where $X_1(t)$ is the deterministic motion of the top cantilever when the step force is removed from the top cantilever, and $X_2(t)$ is the deterministic motion of the bottom cantilever when the step force is removed from the top cantilever. These equations apply in the limit of small perturbations and were recently shown to be valid for the interpretation of correlation force spectroscopy experiments with laterally offset cantilevers in Newtonian fluids by comparison of experiment to finite element modeling of cantilever ringdown.[14,38]

It is known that the correlations in thermal fluctuations of a cantilever can be described quantitatively using a simple harmonic oscillator model.[39] Here, we explore two coupled harmonic oscillators to model the ringdown of the cantilevers, which can then be input into Eqs. (1) and (2) to generate the correlations for comparison to experiment. In this HO model, each cantilever is modeled as a lumped mass, m, connected to the same fixed base by a spring of stiffness, k (the cantilever), and a damper with damping coefficient, γ_a (the hydrodynamic damping on the cantilever), as shown schematically in Fig. 5. We ignore the damping by the material that comprises the cantilever because it is small. The hydrodynamic damping from the fluid spanning the gap between the two cantilevers is modeled as a second damper with damping coefficient, γ_c

$$\ddot{X}_1 + \left(\frac{\gamma_a}{m} + \frac{\gamma_c}{m}\right)\dot{X}_1 - \frac{\gamma_c}{m}\dot{X}_2 + {\omega_r}^2 X_1 = 0, \tag{3}$$

$$\ddot{X}_2 + \left(\frac{\gamma_a}{m} + \frac{\gamma_c}{m}\right)\dot{X}_2 - \frac{\gamma_c}{m}\dot{X}_1 + {\omega_r}^2 X_2 = 0. \tag{4}$$

We expect that γ_c is a function of the fluid, the oscillation frequency, and also the separation between the cantilevers.[14,38] m is the lumped mass which includes the actual mass of the cantilever plus the fluid loaded mass due to the motion of the fluid surrounding the cantilever (the plates shown in the schematic have zero mass). In general, m and

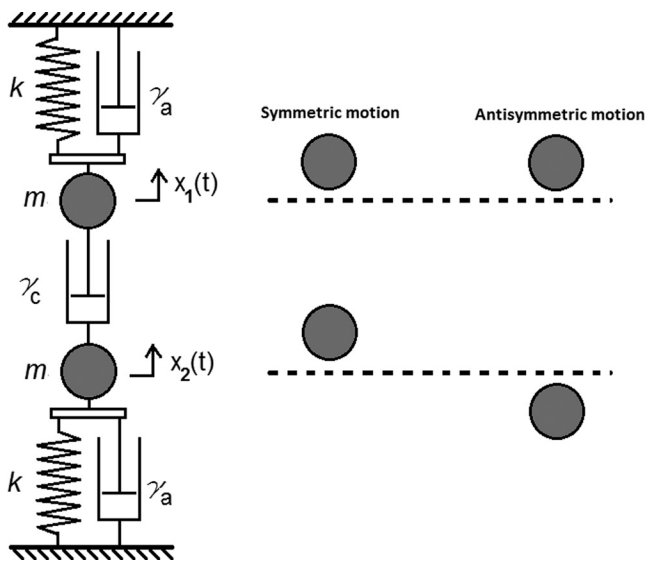

FIG. 5. Our model for the cantilever mechanics in a Newtonian fluid. m is the effective fluid loaded mass of the cantilever, k is the spring constant, and γ_a is the hydrodynamic damping on individual cantilevers. γ_c is hydrodynamic damping from fluid spanning in the gap between the two cantilevers.

γ_a (and γ_c) are frequency-dependent parameters (see Eqs. (28) and (29) in Ref. 35); however, for computational simplicity in our HO model we assume that they are constant for the resonance peak that we analyze. Thus, we expect that the HO model will be more accurate for fluids with narrower resonant frequency, i.e., higher Q factor.[14] We fit γ_a and ω_r from the autocorrelation of one of the cantilevers when the two cantilevers are far from each other. At large separations, all the damping is attributed to γ_a, and thus $\gamma_c = 0$.

Thus, we obtain all three parameters γ_a, m, and k from experimental measurements of the autocorrelation of cantilever displacement in water at large separation, and the parameter of interest, γ_c, is fit for each individual separation. γ_a and ω_r are kept constant for the rest of separations and the only fitting parameter is γ_c.The lumped mass in fluid for each cantilever was obtained from the resonant frequency in the fluid, ω_r, and the stiffness of the cantilever using $m = k/{\omega_r}^2$.

The initial conditions of the ringdown are $X_1(0) = F_1/k$ (the initial step force), and $X_2 = \dot{X}_1 = \dot{X}_2 = 0$ from experimental data. Since all motions are scaled by the magnitude of the initial step force, from here on we present all equations and results with displacements nondimensionalized by F_1/k. The solution to Eqs. (3) and (4) in symmetric and antisymmetric modes is[14]

$$X_s(t) = \exp\left(\frac{-\gamma_a}{2m}t\right)\left(\cos\left(\sqrt{{\omega_r}^2 - \left(\frac{\gamma_a}{2m}\right)^2}\,t\right) + \frac{\left(\frac{\gamma_a}{2m}\right)}{\sqrt{{\omega_r}^2 - \left(\frac{\gamma_a}{2m}\right)^2}}\sin\left(\sqrt{{\omega_r}^2 - \left(\frac{\gamma_a}{2m}\right)^2}\,t\right)\right), \quad (5)$$

$$X_a(t) = \exp\left(-\left(\frac{\gamma_a}{2m}+\frac{\gamma_c}{m}\right)t\right) \times \left(\cos\left(\sqrt{{\omega_r}^2 - \left(\frac{\gamma_a}{2m}+\frac{\gamma_c}{m}\right)^2}\,t\right) - \frac{-\left(\frac{\gamma_a}{2m}+\frac{\gamma_c}{m}\right)}{\sqrt{{\omega_r}^2 - \left(\frac{\gamma_a}{2m}+\frac{\gamma_c}{m}\right)^2}}\sin\left(\sqrt{{\omega_r}^2 - \left(\frac{\gamma_a}{2m}+\frac{\gamma_c}{m}\right)^2}\,t\right)\right). \quad (6)$$

The motion of the cantilevers are then $X_1 = (X_s + X_a)/2$ and $X_2 = (X_s - X_a)/2$. Comparing the two modes, it is obvious that the presence of the damper γ_c does nothing to the symmetric mode, but speeds the decay and decreases the oscillation frequency in the antisymmetric mode.

The best fit for γ_c was obtained by minimizing the deviation squared between the measured cross-correlation and the cross-correlation from the HO model over the range 0 to 1 ms in Fig. 4. We also examined the best fit to both the cross-correlation and the autocorrelation together, which produced essentially the same results.

The HO fit is shown in Fig. 6 together with the experimental data for water at several cantilever-cantilever distances. The HO fit is very good for cantilever separations out to about 8 μm but is not so good at a cantilever separation of 13.5 μm. The diminished quality of the fit at large separation may be because the cross-correlation is weaker and the fluid coupling is small. However, the agreement between theory and experiment is very good at the small separations, which is the important region in single molecule spectroscopy. Thus, we have set the base model to which the properties of a straddling molecule can be added.

The absolute values of the fit parameters are also of interest. First, the fitted value of $\gamma_a = 14.8 \times 10^{-7}$ kg/s (obtained at large separation and held constant for other separations) is similar to the value calculated at the resonant frequency from a harmonic oscillator model using frequency-dependent damping $\gamma_a = 16.5 \times 10^{-7}$ kg/s[39,40] (Eq. (29) in Ref. 35). A fluid with greater damping (and thus a larger spread of frequencies at resonance) would be expected to return poorer agreement than water ($Q = 2.3$).

Fitted values of the hydrodynamic coupling as a function of separation are shown in Fig. 7. For small separations ($s = 318$–1000 nm), γ_c is almost constant and these are the separations of interest in molecule force spectroscopy.[41,42] As described above, the roughly constant value of γ_c means that there will be one fewer parameters to fit as a function of separation. At these separations γ_c is about 2 times smaller than γ_a which demonstrates the advantage of measuring the cross-correlated motion of two cantilevers, compared to one cantilever. At separations greater than 1000 nm, γ_c diminishes monotonically and is approximately linear with separation until it is about an order of magnitude smaller than γ_a (at a separation of about 13 μm).

V. PREDICTED RESOLUTION OF SINGLE MOLECULE CFS

The magnitude of the *force noise amplitude*, F_{ij}, can be estimated from the auto and cross-correlations[3,35]

$$F_{ij} = k\sqrt{|\langle x_i(0)x_j(t)\rangle|_{\max}}, \quad (7)$$

where $i = j$ for the single cantilever measurement. The force noise amplitude will depend in general on the separation between the cantilevers and the spring constant. For the experiment in water, the spring constant is $\sim$0.1 N m^{-1} and the maximum amplitude of the cross-correlation is $\sim$0.0051 nm^2, so $F_{12} \sim 8$ pN when the cantilevers are separated by $d = 6.5$ μm ($s = 318$ nm). For a single cantilever of the same spring constant, the thermal noise is about $F_{11} \sim 20$ pN; thus, the thermal noise is about 2.5 times smaller in the two cantilever experiment. Note that we converted the normalized correlations to units of nm^2 through multiplication by k_BT/k.

Figure 8 shows the noise force amplitude, F_{12}, as a function of separation between the two cantilevers. Obviously F_{12} decreases with increasing separation between the two cantilevers. This suggests the use of cantilevers with longer tips in single molecule experiments to reduce the thermal force noise amplitude. In addition to thermal noise, we note also that the use of two (sharp) tips in CFS compared with one tip acting against a plate in one-cantilever single molecule force spectroscopy greatly reduces the van der Waals force in CFS. This is significant because the van der Waals

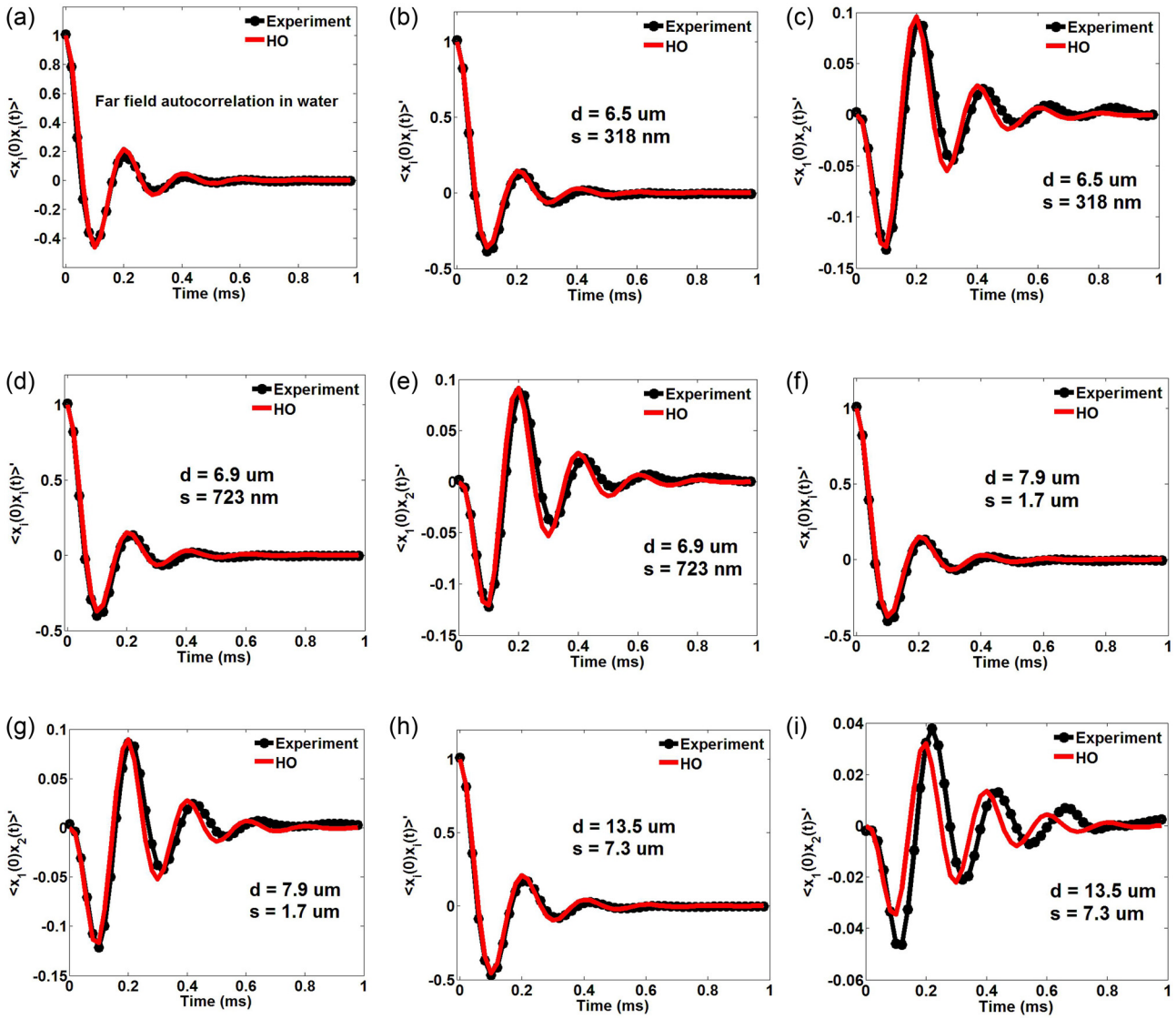

FIG. 6. Auto and cross-correlation of equilibrium fluctuations in cantilever displacement for a pair of AFM cantilevers in water at 23 °C. (a) Autocorrelation at large separation; (b), (d), (f), and (h) autocorrelations for a series of separations; (c), (e), (g), and (i) cross-correlations for a series of separations. Commercial AFM cantilevers are used (ORC8 B: length = 200 μm, width = 40 μm, k = 0.1 N m^{-1}). Experiment is the data measured by CFS, and HO model was calculated using the fluctuation-dissipation (FD) theory to model fluctuations via cantilever ringdown and a coupled HO model for the ringdown (see Eqs. (5) and (6)). The prime on the left axis indicates normalized correlation function. Experimental data collected with Asylum Research Controller at 50 kHz.

forces cause adhesion of two solids and sets a background force that is not of interest in single molecule studies.

VI. SINGLE MOLECULE MEASUREMENTS ON DEXTRAN

The capabilities of the instrument were demonstrated by a measurement of the stiffness and damping of dextran molecules in aqueous solution. The top cantilever tip was immersed into a (10% w/v) solution of dextran (Sigma-Aldrich; part no. 31392; MW = 500 000) in water and then removed and the water allowed to evaporate. The cantilever was washed with a copious amount of water to release loosely attached dextran. The two cantilevers were then placed in the CFS and a drop of water added. In each force run, the top cantilever was brought into contact with the bottom cantilever, and dwelled for a few seconds at a few nN contact force. It was then retracted from the bottom

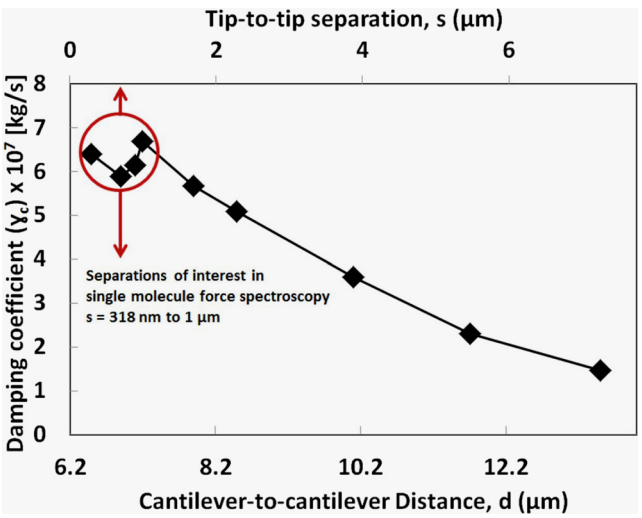

FIG. 7. Fitted damping coefficient γ_c as a function of separation between the cantilevers. Fits are shown in Fig. 6. For comparison $\gamma_a = 14.8 \times 10^{-7}$ kg/s.

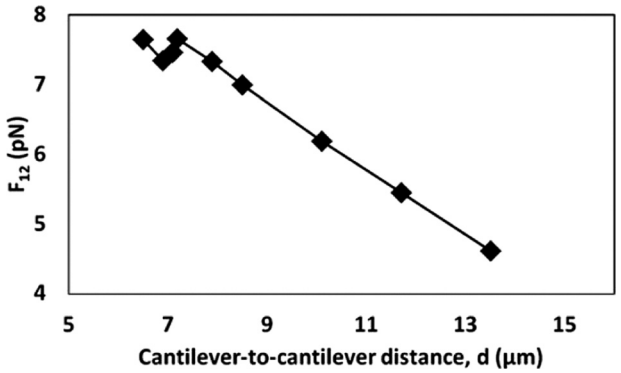

FIG. 8. The noise force amplitude due to fluid coupling (F_{12}) versus distance between the two cantilevers. Maximum of cross-correlations, $|\langle x_1(0)x_2(t)\rangle|_{max}$, are obtained from Fig. 6.

cantilever by increasing the separation between the bases of the cantilevers at a constant velocity while the NI-card recorded the deflection signals from each cantilever at 1 MHz. Sample deflection signals are shown in Fig. 9. The optical lever sensitivity (OLS) of each cantilever was calculated using the spring constant of the cantilever (measured earlier by the thermal method) combined with a thermal noise spectrum at the end of each run (with tips not touching). The measurements in Fig. 9 show that each cantilever senses an approximately equal and opposite force as required for a system near mechanical equilibrium.

The fluctuation spectrum depends on what is tethered between the two cantilevers. The interesting time window for single molecule measurements is the last (largest separation) region where the cantilever is deflected before a mechanical instability (see Figure 9); for that region only a single polymer still straddles between the tips. The fluctuations in this region were divided into displacement segments so that the polymer properties could be analyzed as a function of polymer extension.

The fluctuations were again analyzed using HO modeling but this time the term, γ_c, has been divided into two contributions, $\gamma_{c,p}$ (polymer damping) and $\gamma_{c,fl}$ (fluid damping). The polymer stiffness, k_p, has also been added. The polymer damping, which is sometimes called the internal friction, is the additional damping that arises from the presence of the polymer and includes dissipation caused by the polymer moving through the solvent and through itself. First, the fluctuations were fitted after the polymer bridge was broken to determine the parameters except for $\gamma_{c,p}$ and k_p.

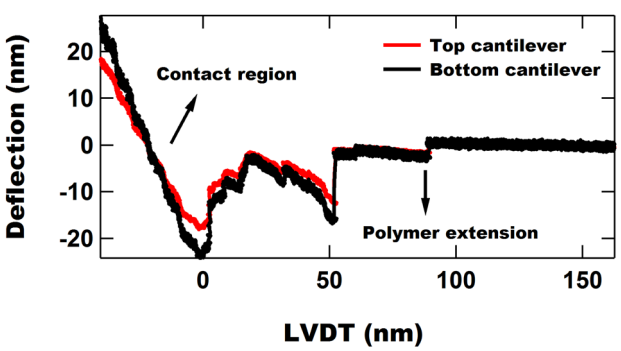

FIG. 9. Deflection of top and bottom cantilevers. The deflection signal has been filtered at 500 Hz to remove noise.

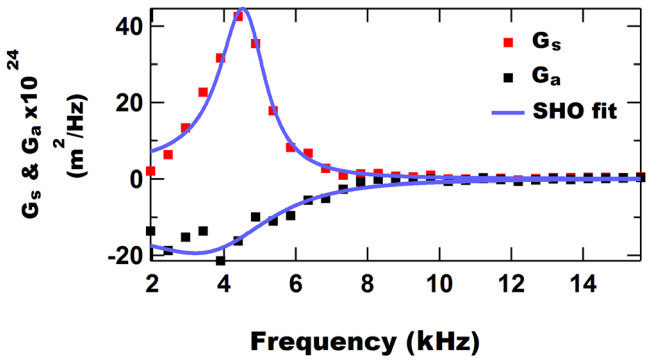

FIG. 10. Fits of Eqs. (8) and (9) to the measured thermal noise spectrum at a tip–tip separation of 152 nm with polymer straddling between the tips (the same polymer extension shown in Fig. 9). The drift during this measurement was about 1 nm/s, and each displacement segment is 0.3 s, so the drift for each segment is 0.3 nm. Fitted values are $\gamma_{c,p} = 164\ \mu g/s$ and $k_p = 2.9$ mN/m.

Then, the fluctuations during polymer extension were fitted to the following equations to obtain $\gamma_{c,p}$ and k_p:

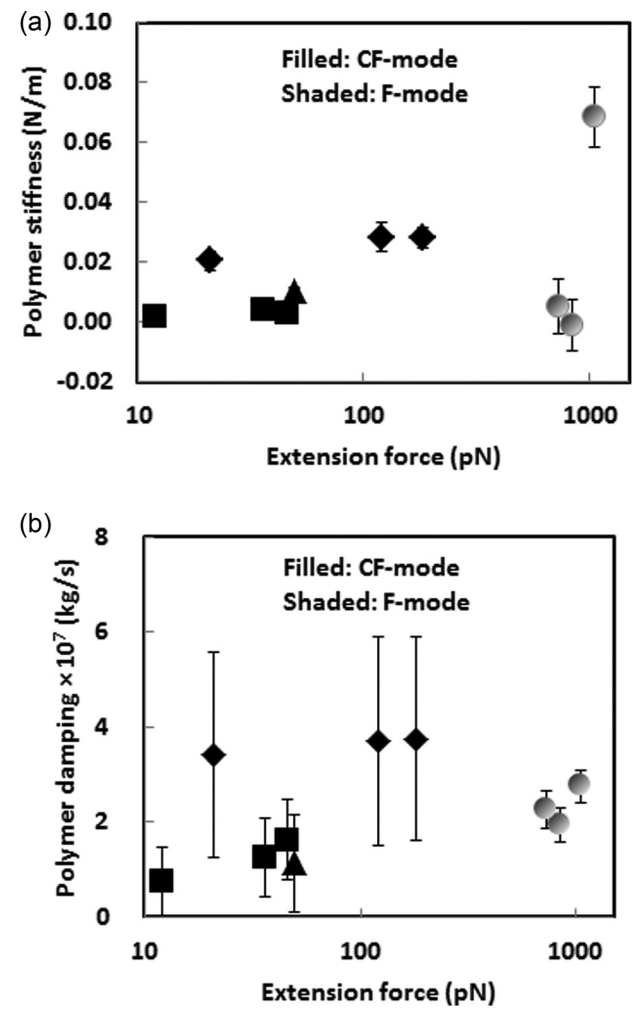

FIG. 11. Parameters used to fit Eqs. (8) and (9) to measured fluctuation data during extension of a dextran molecule. CFS data (correlated fluctuations mode or CF-mode) symbols are filled and single cantilever data using the method of Ref. 27 (fluctuations mode or F-mode) are shown by shaded symbols. Different shapes represent different experiments.

$$G_{\mathrm{s,polymert}}(\omega) = \left(\frac{k+2k_p}{k+k_p}\right)\frac{4k_BT\gamma_a}{(m(2\pi\omega)^2-k)^2+(\gamma_a)^2(2\pi\omega)^2}, \tag{8}$$

$$G_{\mathrm{a,polymert}}(\omega) = \left(\frac{k+2k_p}{k+k_p}\right) \times \frac{4k_BT(\gamma_a+2\gamma_{c,fl}+2\gamma_{c,p})}{(m(2\pi\omega)^2-k-2k_p)^2+(\gamma_a+2\gamma_{c,fl}+2\gamma_{c,p})^2(2\pi\omega)^2}, \tag{9}$$

where the subscript s denotes the symmetric mode, and a denotes the antisymmetric mode. (Note that the noise spectra and correlation functions are Fourier transforms of each other, see Eqs. (13) and (14) in Ref. 35.) The important point is that $\gamma_{c,fl}$ and $\gamma_{c,p}$ do not appear in Eq. (8) which is a reduction in the number of fitting parameters. A sample fit is shown in Fig. 10.

The fitted values of $\gamma_{c,p}$ and k_p as a function of extension force are shown in Fig. 11. They show that the polymer becomes stiffer as it is extended. For a new type of measurement, it is useful to validate against an existing method. The only other method for measuring internal damping of a single polymer chain (that we are aware of) is the method from Smith's group:[27] We have used their method to obtain data for the same dextran sample and have plotted that data on the same graph for comparison. The measurements using Smith's method are for greater extension force, but our measurements using CFS have a similar magnitude.

VII. CONCLUSIONS

We have developed an instrument that measures the cross-correlation in the thermal vibrations of two closely spaced cantilevers in a tip to tip orientation in fluid at equilibrium. The instrument is easy to incorporate into a commercial AFM and retains the full functionality of the AFM, including imaging and control of cantilever displacement.

Thermal noise sets a fundamental limit to AFM single molecule force resolution. We demonstrated that the CFS has a lower noise floor than single cantilever measurements, and show that the force noise amplitude is already only 8 pN in our current set-up, which is approximately 1/4 of the noise in the one-cantilever spectroscopy using the same cantilever and fluid. The decreased noise arises because the noise along the length of each cantilever is not correlated, only the noise arising from fluid motion in the gap between the cantilevers is correlated.

The correlations in thermal fluctuations of two cantilevers can be described quantitatively using a simple harmonic oscillator model and the fluctuation-dissipation theorem. In our approach, the fit parameters (e.g., damping and stiffness) can be used to understand the properties of fluids or molecules that are between the cantilevers. Fluid damping in the gap between the two cantilevers decreases with increasing separation. However, at small tip-to-tip separations ($<1\ \mu$m), which is the relevant length scale in single molecule spectroscopy, fluid damping between the two cantilevers is almost independent of separation. Thus, in single molecule spectroscopy, the changes in damping can be attributed to the straddling molecule.

CFS can be used to obtain information about single polymer molecules. For example, the fluctuations of cantilevers that are linked by a dextran molecule show that the dextran molecule has a stiffness of about $0.015\ \mathrm{N\ m^{-1}}$ and an internal damping of about 2×10^{-7}kg/s when subject to a force up to 200 pN.

ACKNOWLEDGMENTS

The work described in this paper was funded by the National Science Foundation via Award Number CBET-0959228 and by Virginia Tech. The authors acknowledge useful discussions with Brian Robbins and Dongjin Seo.

[1]J. C. Meiners and S. R. Quake, Phys. Rev. Lett. **82**(10), 2211–2214 (1999).
[2]L. A. Hough and H. D. Ou-Yang, Phys. Rev. E **65**(2), 021906 (2002).
[3]M. T. Clark and M. R. Paul, Int. J. Non-Linear Mech. **42**(4), 690–696 (2007).
[4]P. Bartlett, S. I. Henderson, and S. J. Mitchell, Philos. Trans. R. Soc. London, Ser. A **359**, 883–893 (2001).
[5]M. R. Paul and M. C. Cross, Phys. Rev. Lett. **92**(23), 235501 (2004).
[6]J. Apgar, Y. Tseng, E. Fedorov, M. B. Herwig, S. C. Almo, and D. Wirtz, Biophys. J. **79**(2), 1095–1106 (2000).
[7]T. G. Mason and D. A. Weitz, Phys. Rev. Lett. **75** (14), 2770–2773 (1995).
[8]J. C. Crocker, M. T. Valentine, E. R. Weeks, T. Gisler, P. D. Kaplan, A. G. Yodh, and D. A. Weitz, Phys. Rev. Lett. **85**(4), 888–891 (2000).
[9]D. T. Chen, E. R. Weeks, J. C. Crocker, M. F. Islam, R. Verma, J. Gruber, A. J. Levine, T. C. Lubensky, and A. G. Yodh, Phys. Rev. Lett. **90**(10), 108301 (2003).
[10]F. Gittes, B. Schnurr, P. D. Olmsted, F. C. MacKintosh, and C. F. Schmidt, Phys. Rev. Lett. **79**(17), 3286–3289 (1997).
[11]M. Atakhorrami, J. I. Sulkowska, K. M. Addas, G. H. Koenderink, J. X. Tang, A. J. Levine, F. C. MacKintosh, and C. F. Schmidt, Phys. Rev. E **73**(6), 061501 (2006).
[12]M. Atakhorrami, G. H. Koenderink, C. F. Schmidt, and F. C. MacKintosh, Phys. Rev. Lett. **95**(20), 208302 (2005).
[13]M. Buchanan, M. Atakhorrami, J. F. Palierne, and C. F. Schmidt, Macromolecules **38**(21), 8840–8844 (2005).
[14]M. Radiom, B. Robbins, C. D. F. Honig, J. Y. Walz, M. R. Paul, and W. A. Ducker, Rev. Sci. Instrum. **83**(4), 043908 (2012).
[15]J. C. Meiners and S. R. Quake, Phys. Rev. Lett. **84**(21), 5014 (2000).
[16]X. R. Bao, H. J. Lee, and S. R. Quake, Phys. Rev. Lett. **91**(26), 265506 (2003).
[17]M. Salomo, K. Kroy, K. Kegler, C. Gutsche, M. Struhalla, J. Reinmuth, W. Skokov, C. Immisch, U. Hahn, and F. Kremer, J. Mol. Biol. **359**(3), 769–776 (2006).
[18]M. Salomo, K. Kegler, C. Gutsche, M. Struhalla, J. Reinmuth, W. Skokow, U. Hahn, and F. Kremer, Colloid Polym. Sci. **284**(11), 1325–1331 (2006).
[19]Y. F. Chen, G. A. Blab, and J. C. Meiners, Biophys. J. **96**(11), 4701–4708 (2009).
[20]K. Kegler, M. Salomo, and F. Kremer, Phys. Rev. Lett. **98**(5), 058304 (2007).
[21]A. Idiris, S. Kidoaki, K. Usui, T. Maki, H. Suzuki, M. Ito, M. Aoki, Y. Hayashizaki, and T. Matsuda, Biomacromolecules **6**(5), 2776–2784 (2005).
[22]P. Hinterdorfer, W. Baumgartner, H. J. Gruber, K. Schilcher, and H. Schindler, Proc. Natl. Acad. Sci. U.S.A. **93**(8), 3477–3481 (1996).
[23]G. U. Lee, L. A. Chrisey, and R. J. Colton, Science **266**(5186), 771–773 (1994).
[24]M. Rief, M. Gautel, F. Oesterhelt, J. M. Fernandez, and H. E. Gaub, Science **276**(5315), 1109–1112 (1997).
[25]T. E. Fisher, P. E. Marszalek, and J. M. Fernandez, Nat. Struct. Biol. **7**(9), 719–724 (2000).
[26]H. Clausen-Schaumann, M. Seitz, R. Krautbauer, and H. E. Gaub, Curr. Opin. Chem. Biol. **4**(5), 524–530 (2000).
[27]M. Kawakami, K. Byrne, B. Khatri, T. C. B. McLeish, S. E. Radford, and D. A. Smith, Langmuir **20**(21), 9299–9303 (2004).

[28]M. Kawakami, K. Byrne, B. S. Khatri, T. C. B. McLeish, S. E. Radford, and D. A. Smith, Langmuir **21**(10), 4765–4772 (2005).
[29]M. Kawakami, K. Byrne, B. S. Khatri, T. C. B. McLeish, and D. A. Smith, ChemPhysPhys **7**(8), 1710–1716 (2006).
[30]M. T. Clark and M. R. Paul, J. Appl. Phys. **103**, 094910 (2008).
[31]C. P. Green and J. E. Sader, J. Appl. Phys. **98**, 114913 (2005).
[32]G. Meyer and N. M. Amer, Appl. Phys. Lett. **53**, 1045–1047 (1988).
[33]W. A. Ducker, T. J. Senden, and R. M. Pashley, Langmuir **8**(7), 1831–1836 (1992).
[34]J. L. Arlett, M. R. Paul, J. Solomon, M. C. Cross, S. E. Fraser, and M. L. Roukes, Lect. Notes Phys. **711**, 241–270 (2007).
[35]M. R. Paul, M. T. Clark, and M. C. Cross, Nanotechnology **17**(17), 4502–4513 (2006).
[36]S. Henderson, S. Mitchell, and P. Bartlett, Phys. Rev. E **64**(6), 061403 (2001).
[37]D. Chandler, *Introduction to Modern Statistical Mechanics* (Oxford University Press, 1987), pp. 234–271.
[38]C. D. F. Honig, M. Radiom, B. Robbins, J. Y. Walz, M. P. Paul, and W. A. Ducker, Appl. Phys. Lett. **100**, 053121 (2012).
[39]J. E. Sader, J. Appl. Phys. **84**(1), 64–76 (1998).
[40]J. W. M. Chon, P. Mulvaney, and J. E. Sader, J. Appl. Phys. **87**(8), 3978–3988 (2000).
[41]H. B. Li, B. B. Liu, X. Zhang, C. X. Gao, J. C. Shen, and G. T. Zou, Langmuir **15**(6), 2120–2124 (1999).
[42]H. B. Li, W. K. Zhang, W. Q. Xu, and X. Zhang, Macromolecules **33**(2), 465–469 (2000).